11th International Conference on Fast Sea Transportation
FAST 2011, Honolulu, Hawaii, USA, September 2011

# Time-Domain Seakeeping Simulations for a High Speed Catamaran with an Active Ride Control System

Michael J. Hughes[1] and Kenneth M. Weems[2]

[1]Naval Surface Warfare Center, Carderock Division, West Bethesda, Maryland, USA
[2]Science Applications International Corporation, Bowie, Maryland, USA

## ABSTRACT

This paper describes time-domain seakeeping simulations for a high speed wave piercing catamaran with an active ride control system, and the validation of the simulations using data from full-scale sea trials. The simulations are performed using the Large Amplitude Motion Program (LAMP), a time-domain potential flow panel code that solves the 3-D wave-body hydrodynamics and rigid-body dynamics problems. The lift forces produced by ride control devices such as trim tabs, interceptors, and foils are modeled as external forces in the time-domain simulation. The paper describes several modifications to the modeling of active ride control systems in LAMP, including the development of new models for the lift forces on trim tabs and interceptors. Validation studies have been performed with LAMP for catamarans without ride control systems (Zhang et al. 2003), but there has been very little validation of the program for vessels with active ride control systems, in part because the availability of suitable seakeeping data for high speed vessels with active ride control systems is very limited. Seakeeping model tests are usually performed without active ride control systems because the small size of model-scale fins, trim tabs, and/or interceptors would result in significant scaling effects, thereby limiting their value. When using data from full-scale trials for validation, the uncertainties relating to the direction and variability of the wave field can be considerable. The details of the ride control algorithm and gain settings used during the trials were unknown, but the time history of the trim tab and T-foil deflection angles were recorded. The general PID control algorithm in LAMP was used with the controller gains adjusted to match the RMS foil and tab deflection angles measured during the trials. The results from the time-domain simulations are also compared with previously published simulations from frequency domain seakeeping simulations of the same catamaran and active ride control system performed using the VERES seakeeping code (Hughes 2010). The LAMP time-domain simulations are able to model some non-linear aspects of the ride control system that cannot be modeled in a linear frequency domain simulation, such as the nonlinear lift curve for interceptors and the reduction in lift on foils from stall and cavitation inception.

## KEY WORDS

Ride Control, Seakeeping, Catamaran, CFD

## 1.0 INTRODUCTION

High-speed multihull vessels, with very few exceptions, utilize active ride control systems (RCS) to reduce motions in higher sea states. These types of vessels are commonly used as high-speed ferries where the RCS is used to improve passenger comfort. In recent years, the US Navy has also developed an interest in high-speed multihull vessels for use as inter-theater transport vessels or littoral combat ships. Computational seakeeping simulation tools can be used to aid the design of these vessels and develop operator guidance for these vessels for naval applications. The RCS can have a significant influence on the vessel motions, so it is important that the computational tools accurately model the RCS. In many cases the ride control algorithms used to control deflections of the lift devices are proprietary, so while information is usually available describing the geometry of the lift devices, no information is typically available regarding the algorithm or gain settings used by an RCS. Using computational tools to predict the motions of these vessels without knowing the control algorithm or gain settings used by the RCS requires a number of assumptions. This paper describes the modeling of a vessel with a general PID control algorithm in the simulation tool LAMP. The principal assumption is that if the generic RCS model produces the same RMS deflections of the lift devises as the actual RCS, reasonable predictions of the benefits of the RCS will be attained. The methods described to estimate the control algorithm can also be used to evaluate the effect of RCS devices during preliminary design, before the details of the actual RCS are determined.

The Navy has several tools available to predict the seakeeping performance of high-speed multihull vessels, ranging from a strip theory tool (VERES) to 3-D boundary element methods (LAMP and AEGIR), and Unsteady RANS methods such as CFDShip-Iowa. These tools have been compared with model test data for high-speed catamarans and trimarans without ride control systems, and in general good correlation has been shown. Comparisons of VERES predictions to model tests for several high-speed multihull vessels can be found in O'Dea (2005). Stern et al. (2006) show comparisons of predictions from VERES, AEGIR and CFDShip-Iowa to model test data for a high-speed catamaran. Zhang et al. (2003) shows the correlation of LAMP predictions with model test data for the same case. There has been little work done to correlate the predictions from the tools with data for a vessel with an active RCS. Hart et al. (2007) compared LAMP predictions to trials data

for a lifting body technology demonstrator that included a dynamic ride control system. The principal problem is that the data available for the validation of the seakeeping performance of high-speed vessels with active ride control systems is very limited. Seakeeping model tests are usually performed without active ride control systems, in part because the small size of the model-scale fins, trim tabs and/or interceptors would result in significant scaling effects, which would limit the value of including active ride control systems in model tests. In this paper the data from the full-scale trials of a wave piercing catamaran (Fig. 1) are used to compare with the predictions from section.

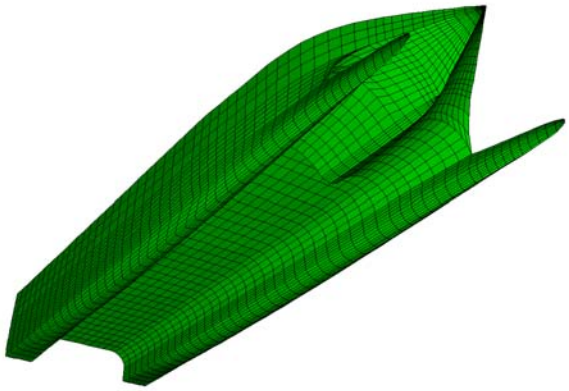

**Fig. 1.** Hull geometry model of wave piercing catamaran.

## 2.0 Modeling Ride Control Systems in LAMP

### 2.1 Ride Control System Basics

The ride control system on a typical high-speed catamaran is shown schematically in Fig. 2.

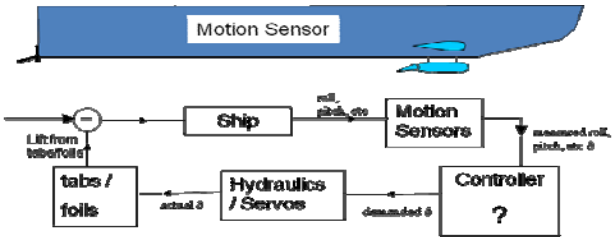


**Fig. 2.** Ride Control System Schematic.

At the stern there are a set of lifting devices while another set of lifting devices is located forward, typically about 20-30% of the length from the bow. The aft lift effectors can be either trim tabs or interceptors mounted to the transom of each hull. The forward lift effectors can be a set of fins mounted flush with each hull, T-foils mounted below each hull or a single larger T-foil mounted on a strut attached to the wetdeck on the centerline of the vessel. The foils may be either all movable or have movable flaps. A set of motion sensors incorporating accelerometers, inclinometers and rate gyros are installed in order to measure the motions of the ship and provide feedback to the control algorithm. The control algorithm computes the desired deflections of the lifting devices in order to reduce the unsteady motions of the vessel. Hydraulic or electric actuators are then used to deflect the fins, foils, trim tabs and/or interceptors. The question mark in the box representing the controller in Fig. 2 indicates that the details of the control algorithm are often proprietary and therefore not available to an engineer performing a seakeeping analysis.

### 2.2 The LAMP Program

LAMP is a nonlinear time-domain potential flow seakeeping code developed to predict the motions and loads of a ship or other marine vehicle in a seaway. LAMP was originally developed supplement traditional frequency-domain methods in the prediction of nonlinear hull loads of large naval combatants and commercial ships in severe sea conditions. Since then, LAMP's time-domain approach, 3-D geometry model, nonlinear hydrodynamics, and flexible external force and system models have allowed it to be used for the analysis of a wide variety of conventional and unconventional ships and marine vehicles including tumblehome and multi-hull ships, high-speed displacement hulls, buoys, and offshore platforms (Shin et al. 2003).

At LAMP's core is a time-domain potential-flow solution of the ship-wave hydrodynamic interaction problem, for which several solution "levels" and formulations have been implemented. The present analysis uses the approximate body-nonlinear method in which the incident wave force (Froude-Krylov) and hydrostatic pressure are integrated over the instantaneous wetted hull surface up to the incident wave, while the wave-body disturbance forces, which includes radiation, diffraction and forward speed effects, are calculated over the mean wetted hull surface. A disturbance velocity potential is calculated using a 3-D Rankine singularity potential flow panel method which solves a combined body boundary condition over the mean wetted hull surface, a linearized free surface boundary condition over a local portion of the free surface and a numerical radiation condition at the outer edge of the free surface. Bernoulli's equation including the 2nd order velocity terms is used to get the pressure, which is integrated over the hull surface to get the hydrodynamic forces. Additional waterline terms are added to complete the 2nd order forces including drifting effects (Zhang et al. 2009). This "hybrid" calculation approach allows the principal nonlinear effects on ship motions and loads to be captured without the computation cost of a full nonlinear solution.

Since LAMP's potential-flow solution of the wave-body interaction problem does not implicitly include viscous or lifting effects, a series of external force models have been implemented in order to account for viscous drag and damping, propulsion, hull maneuvering forces, anti-rolling tanks and appendages such as rudders, bilge keels and control fins. The appendage lift and drag model are particularly important to the present study and are described in more detail below.

### 2.3 Computing RCS Lift Forces

Many numerical seakeeping tools, including both LAMP and VERES, model control surfaces such as anti-roll fins, T-foils and trim tabs use force models that a) evaluate the

inflow to the control surface from the unsteady ship motion and orbital wave velocity, b) calculate the forces generated by these devices using relatively simple formulae and c) apply them as external forces, which are added to the forces computed from the hydrodynamic calculations. The details of the flow around the control surfaces themselves are not computed, and the control surface geometry is not included in the panel model. The forces usually include the lift, induced drag, and skin frication and can also include an added mass estimate based on the planform area and the formula for the added mass from a flat plate.

In LAMP, these appendage models can be used both for large appendages that are included in the potential flow panel model, such as lifting body for the *Sea Flyer* calculations described in Hart et al. (2007), and for smaller appendages that are not panelized, such as the rudder in a typical ship calculation.

LAMP's lift models include built-in expressions based on the appendage geometry plus an option to enter lift curve data. In the lift calculation, the vector inflow velocity to each appendage is computed by evaluating the relative velocity of an appendage reference point from the ship's rigid body motion plus the orbital velocity of the incident wave field. The geometry of the appendage plus any appendage deflections are used to resolve the velocity into chord-wise, span-wise, and normal components from which an effective inflow velocity, V, and angle of attack, α, can be derived. For long or large appendages, this evaluation can be performed at multiple span-wise locations, primarily in order to account for the variation in inflow velocity vector due to roll velocity.

#### 2.3.1 Basic Lift

The basic lift model, equations (1) through (3), uses the standard expressions for the lift generated by low aspect ratio fully movable foils as presented in Principles of Naval Architecture (Comstock ed. 1967) and other standard texts:

$$Lift = C_{L\alpha}\,{}^{1}\!/\!_{2}\,\rho V^2 A_P \alpha \tag{1}$$

$$C_{L\alpha} = \frac{\pi}{2} A_S : \quad A_S < 2.0\,,\ \alpha < \alpha_{stall} \tag{2}$$

$$C_{L\alpha} = \frac{2\pi}{1 + {}^{2}\!/\!_{A_S}} : \quad A_S \geq 2.0\,,\ \alpha < \alpha_{stall} \tag{3}$$

Where, ρ is the water density, $A_P$ is the planform area, and $A_S$ is the effective aspect ratio, which can include ground boarding or end plating. These expressions are used up to a specified stall angle, $\alpha_{stall}$, after which an 'eddy-making' expression is invoked.

#### 2.3.2 Flap Lift

For appendages with full or partial flaps equations (4) through (6), based on von Mises (1945), are used to compute the incremental lift and moment about the foil leading edge:

$$\Delta C_L = 2\delta\left(\phi + \sin\phi - \lambda\phi\right)\Lambda \tag{4}$$

$$\Delta C_M = -\,{}^{1}\!/\!_{2}\,\delta\left(\sin\phi + {}^{1}\!/\!_{2}\sin 2\phi\right)\Lambda \tag{5}$$

$$\phi = \cos^{-1}\left(1 - 2\lambda\right) \tag{6}$$

where λ is the ratio of the flap chord to the foil chord, Λ is the ratio of the flap span to the foil span, and δ is the flap deflection angle.

#### 2.3.3 Lift Effect with Submergence

Foils moving parallel to and near the free surface will experience a loss of lift as they get very close the surface. To account for this, the following expression has been implemented from Faltinsen (2004):

$$C_{L\alpha} = C_{L\alpha}^{deep}\left(\frac{1 + 16\left(h/c\right)^2}{2 + 16\left(h/c\right)^2}\right) \tag{7}$$

where $C_{L\alpha}^{deep}$ deep is the base "deep water" lift slope coefficient, *c* is the chord length and *h* is the submergence of the foil beneath the incident wave surface.

#### 2.3.4 Specified Lift Curve Data

For cases where appendage lift characteristics can be calculated or measured externally, lift data curves or tables can be specified. These data include the appendage's lift, moment about the spanwise vector, and drag relative to a specified reference point and can be specified with respect to the angle of attack, flap deflection angle, and/or submergence beneath the wave surface. For cases where the depth dependence is not explicitly specified, the specified deep water lift data can be used with the submergence correction from equation (7). The specified lift curve data can include a general nonlinear dependence on the angle of attack, deflection angle and submergence, and can provide a detailed model of the loss of lift and increase of drag through stall and the post-stall region.

#### 2.3.5 Lift on Trim Tabs and Interceptors

While extensive test results have been published for conventional foils, less empirical data are available for the lift generated by trim tabs and interceptors. Some studies have examined the steady force produced by a trim tab or interceptor in calm water to control trim. Savitsky and Brown (1975) derived a formulation to estimate the force on a trim tab hinged under the bottom of a planing hull. More recently Dawson and Blount (2002) developed a procedure to estimate the force on an interceptor by using the Savitsky and Brown (1975) equation for the force on a trim tab and developing a relation between the equivalent vertical movement of the interceptor plate and the deflection angle of the trim tab flap. Villa and Brizzolara (2009) used CFD to develop similar expressions for the forces on both trim

tabs and interceptors. A background presentation prepared for NSWCCD by Maritime Dynamics, Inc, (MDI 2003b, now part of Naiad Dynamics, Inc.) on RCS simulations provided the following formula for use as a simple estimate of the lift slope coefficient per degree of deflection of a trim tab:

$$C_{L\alpha} = \frac{1}{10 * \left(1 + {}^{1}\!/\!_{A_S}\right)^2} \tag{8}$$

The MDI presentation suggested using Equation (8) when more detailed CFD analysis or empirical data are not available for the trim tab, and suggested approximating the lift on an interceptor as 60% of the lift on a trim tab with an equivalent span and an aspect ratio of 2.0. In the current work, Equation (8) is used to estimate $C_{L\alpha}$ on trim tabs. It is also assumed in the current work that the lift on the trim tab is proportional only to the deflection angle of the tab, not the total resolved angle of attack to the tab including ship motion and wave orbital velocity as in the case of a foil. This assumption accounts for the influence of the hull straightening the flow into the tab or interceptor.

For trim tabs, it is important to include the added mass force acting on the tab as it flaps up and down. This added mass component of the force can be a significant component of the force generated by the trim tab, particularly at low speeds. LAMP's appendage force model includes an optional added mass calculation which accounts for the normal acceleration due to the unsteady ship motion and unsteady flap deflection.

$$\vec{F}_{adm} = -m_{33}(\ddot{\vec{x}}(\vec{x}_c) \cdot \hat{n} - 0.5 c_{flap} \ddot{\delta}) \tag{8}$$

The normal added mass coefficient of the trim tab is computed using the following formula from Lewandowski (2004):

$$m_{33} = \frac{\rho \pi A_s c^2 s}{4\sqrt{A_s^2 + 1}} \tag{9}$$

The flat plane normal force coefficient from Hoerner (1965) can be used to derive a similar expression a flaps normal drag force due to deflection rate.

$$\vec{F}_{ndrag} = -1.17 \frac{\rho}{2} (0.25\, c_{flap}^2 \dot{\delta} \left|\dot{\delta}\right|) \hat{n} \tag{10}$$

### 2.4 PID Control Algorithm

LAMP includes a general foil control option that is based on a PID (proportional, integral, derivative) algorithm, to compute the commanded deflection of a foil based on feedback from the heave, roll and pitch motion of the vessel. The user supplies the PID gains for each degree of freedom. In the current simulations, it is assumed that the trim tabs and foils are used only to control pitch and roll motions, and the expression for the commanded deflection becomes:

$$\begin{aligned} \delta_c = {} & G_{\theta P}(\theta_d - \theta) + G_{\theta i} \int_0^t (\theta_d - \theta(\tau)) d\tau - G_{\theta d} \dot{\theta} \\ & + G_{\phi P}(\phi_d - \phi) + G_{\phi i} \int_0^t (\phi_d - \phi(\tau)) d\tau - G_{\phi d} \dot{\phi} \end{aligned} \tag{11}$$

where $\delta_c$ is the commanded deflection angle; $G_{\theta P}$, $G_{\theta i}$ and $G_{\theta d}$ are the proportional, integral and derivative gains for pitch control and $G_{\phi P}$, $G_{\phi i}$ and $G_{\phi d}$ are the same gains for roll control. $\theta$, $\theta_d$ and $\dot{\theta}$ are the current value, target value and time derivative of the pitch angle and $\phi$, $\phi_d$ and $\dot{\phi}$ are the current value, target value and time derivative of the roll angle. A fairly simple servo model is used to compute the realized fin or flap deflection at each time step.

In the current study, as well as in many other cases, the ride control algorithms used to control deflections of the lift devices are proprietary. When applying the general PID controller in LAMP to approximate the unknown actual controller, some assumptions must be made. Increasing the proportional gains in the PID formula will increase the stiffness of the vessel in roll and pitch, while increasing the derivative gains will increase the roll and pitch damping. Catamarans are generally fairly stiff in roll and pitch but lightly damped, so the objective of the ride control system is mainly to add additional damping for the roll and pitch motions. Based on this assumption and the analysis of a series of roll and pitch decay simulations in LAMP, the integral gain terms were set to zero, and the ratio of the derivative gain to the proportional gain was set to six. This reduces the number of input coefficients to the control model that must be determined to the overall roll and pitch gains, which are specified as $G_{\phi T}$ and $G_{\theta T}$ in Eqn. (12).

$$\delta_c = G_{\theta T}\left[(\theta_d - \theta) - 6\dot{\theta}\right] + G_{\phi T}\left[(\phi_d - \phi) - 6\dot{\phi}\right] \tag{12}$$

The overall pitch and roll gain coefficients are determined in an iterative manner to achieve the desired RMS deflection of the foil or flap. Simulations in head seas are performed to determine the overall pitch gain and simulations in beam seas are performed to determine the overall roll gain. The simulations are repeated, iteratively adjusting the overall pitch and roll gains until the desired RMS deflection of the control surface is realized. The iterative procedure used to determine the overall pitch and roll gains must be repeated for each sea state examined. Since LAMP uses a linear PID algorithm, the control surface deflection vary roughly linearly with wave height if the gains are left constant, so unrealistic deflections could be computed if the gains are not adjusted for each sea state examined.

The data from the full-scale trials discussed later in this paper included the time history of the trim tab and T-foil flap deflections for each run. For the LAMP calculations performed to correlate with that data, the overall gain coefficients for each device could be adjusted such that the RMS deflections computed in the LAMP simulations are very close to the RMS deflections recorded during the trials.

For design studies, appropriate target RMS deflection values can be estimated from analysis of the foil geometry. Guidance from a study performed by Naiad Dynamics, Inc. for NSWCCD (MDI 2003a, 2003b) and more recent consultations with Naiad Dynamics (Schaub) suggested the following constraints be considered when estimating the RMS deflection angles for various ride control devices:

- Trim tabs should have RMS deflection angles of 4 to 5 degrees for the typical installation. Hydraulic power constraints could limit motions at high speeds.
- Fins and foil RMS motion limits are based on estimates of cavitation inception. The CFD based cavitation inception CL for each speed can be used as a measure of the maximum RMS value thus implying a little cavitation near the maximum angles of the simulation. A typical T-foil might be limited to about 6 degrees RMS at 35 knots and 4.8 degrees RMS at 42 knots.
- The maximum deflection angle limits based on mechanical constraints are approximately 10° for the trim tabs, 20° for the T-foils.

## 3.0 Correlation with Full-Scale Trials

### 3.1 Description of Trials

Comparisons are made between the LAMP predictions and data from the full-scale trials for a wave piercing catamaran. The ride control system on the vessel consisted of a pair of trim tabs mounted to the transom of each side hull, and a large T-foil mounted to the wetdeck of the catamaran on the vessel centerline. The T-foil was retractable, so it could be pulled out of the water and stowed beneath the wetdeck. The T-foil had controllable flaps covering about 35% of the chord, and the T-foil strut could also be pivoted to adjust the angle of incidence. In the current analysis, only the flap motion of the T-foil is modeled. Restrictions on the distribution of the full-scale trials data prevent the details of the hull geometry of the wave piercing catamaran from being published here, and the scales on the y-axis of the plots have been removed; however, these restrictions still allow for comparisons between the trials and calculations. The heading convention is such that 0˚ corresponds to head seas, 90˚ to beam seas and 180˚ to following sea.

Correlation with data from full-scale trials is challenging because the description of the incident wave field encountered during the trials is not sufficient to define the incident waves for input to the computer simulation. In the current set of trials, a measurement of the wave spectrum before and after each octagon was performed using a TSK wave height system installed at the bow of the ship. The TSK wave probe provides a point spectrum showing the distribution of wave energy across wave frequencies, but does not indicate the direction of the waves or amount of wave spreading or if the seas are bi-directional. The primary wave direction is observed by the operators and an octagon maneuver is performed as shown in Fig. 3 to obtain data at various headings. In choosing runs to use for the correlation, the pitch and roll response as a function of heading was examined to rule out octagons where there was clearly a strong swell component to the seas in a direction other than the primary wave direction. For providing input into LAMP a spectrum is formed by averaging the measured spectrum recorded at the beginning and end of the octagon maneuver. The resulting spectra obtained for two of the octagons from the trials are shown in Figure 4. The runs referred to as "Octagon A" corresponded to a case where the ship travelled at 20 knots in a high Sea State 4 (HS=2.3m). The runs referred to as "Octagon B" corresponded to a case where the ship travelled at 35 knots in low Sea State 5 (HS=2.7m). For both Octagon A and Octagon B, the T-foil was retracted out of the water and only the trim tabs were used to reduce the vessel motions. The modal period was longer during the Octagon B runs. Both spectra show a secondary peak at a shorter wave period than the modal period.

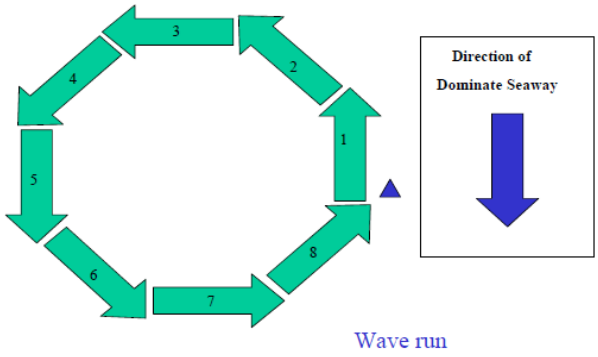


**Fig. 3.** Octagon Maneuver Pattern

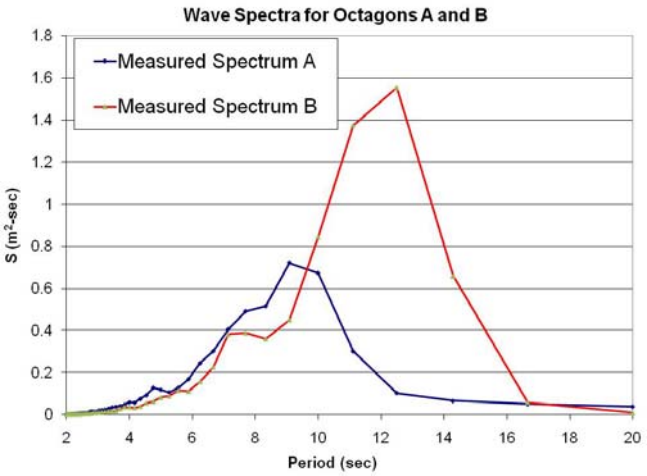


**Fig. 4.** Wave Spectra measured during Octagons A and B

### 3.2 LAMP calculations

The 3-D panel model was generated for the wave piercing catamaran and a portion of the free surface surrounding the catamaran, which is shown in Fig. 5. All of the LAMP simulations were performed using the approximate body-nonlinear approach in which the disturbance potential is computed over the mean wetted surface while the incident

wave forcing and hydrostatic restoring forces are computed over the instantaneous wetted hull surface. The seaway corresponding to each octagon maneuver was specified as a set of 1100 wave components. The amplitudes of the wave components were computed outside of LAMP to reproduce the measured spectrum, using 100 wave frequencies and 11 spreading angles at each frequency. As no information is available for the amount of wave spreading in the waves during the trials, a cos2 spreading function was applied assuming a 90° spreading angle in the LAMP calculations. A random phase value was assigned to each wave component.

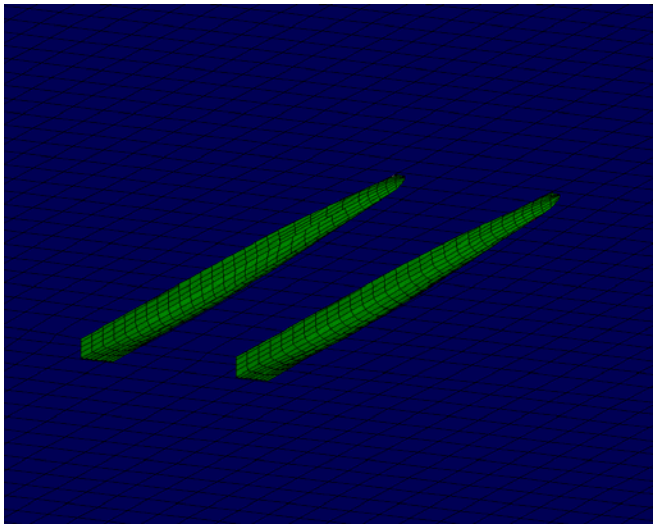

**Fig. 5.** LAMP panel model of wave piercing catamaran .

LAMP simulations were performed in head, bow, beam and stern quartering seas in wave spectrum measured for each octagon. Six minute simulations were performed for each heading from which the RMS motions in each degree of freedom were computed. The waterjets were not modeled as part of the LAMP simulation, which was performed with five degrees of freedom including all modes except surge. As the waterjets were also used for steering, soft springs were included to keep the vessel on course. The forces contributed by the trim tabs included both the lift and added mass force computed using the method discussed in Section 2.3.5, and the PID control gains for each tab was set to reduce the roll and pitch motion following the method described in Section 2.4. The lift on the T-foil, when present, was computed using the default method for the lift on a flapped foil discussed in Sections 2.31 through 2.33. As the T-foil was located on the centerline with a full span flap, it was used only to control the pitch motion and the roll gains were set to zero.

### 3.3 Comparisons

The RMS values for roll and pitch motion predicted by the LAMP calculations are compared both with the measured values from the trials as well as previous calculations using VERES, which are described in Hughes (2010). VERES is a strip theory ship motion prediction code, developed by MARINTEK (Fathi and Hoff, 2004) and (Fathi, 2004). It implements both ordinary strip theory (Salvesen et al., 1970) as well as the high-speed theory of Faltinsen and Zhao (1991). It has the capability of handling both monohull and multihull vessel geometries. The strip theory solves frequency domain equations of motion, to obtain the transfer functions defining the response of the vessel to regular waves at a specified set of frequencies. A postprocessor is used to derive useful statistical information in irregular seas. More details on the theory and use of VERES can be found in (Fathi and Hoff, 2004) and (Fathi, 2004).

The comparison of the predicted motions with the trials data for Octagon A is shown in Figures 6 and 7 for the RMS roll and pitch angle respectively. Predictions were also made for the vessel with no trim tabs (labeled "bare hull" on the plots). The trials were performed with the trim tabs actively controlled. There are no trials data available for this vessel with the trim tabs locked at a fixed angle for any condition. For this case the vessel is travelling at 20 knots and the modal wave period was about 9 seconds. For the bare hull predictions, LAMP and VERES correlate well for the pitch motion, while LAMP predicts a lower RMS roll motion than VERES. The two tools also correlate well with each other for the predicted pitch motion when the trim tabs are modelled and the tools correlate well with the trials data. For this case LAMP predicts a lower RMS roll motion than VERES and both tools under-predict the trials data. For Octagon B the comparisons for the RMS roll and pitch angle are shown in Figures 8 and 9 respectively. or this case the vessel is travelling at a higher speed, 35 knots, in a wave spectrum with a longer modal period of about 12 seconds. The LAMP and VERES predictions correlate fairly well with each other for both pitch and roll motion, and the trials data falls between the predicted results for the bare hull and vessel with actively controlled trim tabs, with the trials data closer to predictions with the trim tabs included for most of the values, particularly for the pitch response.

The VERES predictions are purely linear, whereas the LAMP predictions include some of the important nonlinear aspects; in particular LAMP integrates the hydrostatic and incident wave pressure over the hull up to the instantaneous wave surface. The wave piercing catamaran includes a large wedge shaped center-bow structure under the forward wetdeck, which although above the calm water surface will enter and exit the water in waves and have an influence on the motions. This structure can be seen in Fig. 1. As VERES uses only the geometry up to the calm water surface the influence of this body is not included, while in LAMP this effect is at least partly accounted for through the body nonlinear incident wave forcing and hydrostatic force calculation. Also VERES does not include a specific model for trim tabs and interceptors, so the tabs are modeled as submerged foils, with the lift proportional to the overall angle of attack on the tab, including the influence of wave orbital velocity and ship motion in addition to deflection

 

angle. In the trim tab model in LAMP, the lift on the trim tab is proportional only to the tab deflection angle. Considering the nonlinear effects included in LAMP but not included in VERES, the difference in the predictions between the two codes is about what should be expected. Both tools predict reduced pitch and roll motion with the trim tabs active compared with the bare hull response.

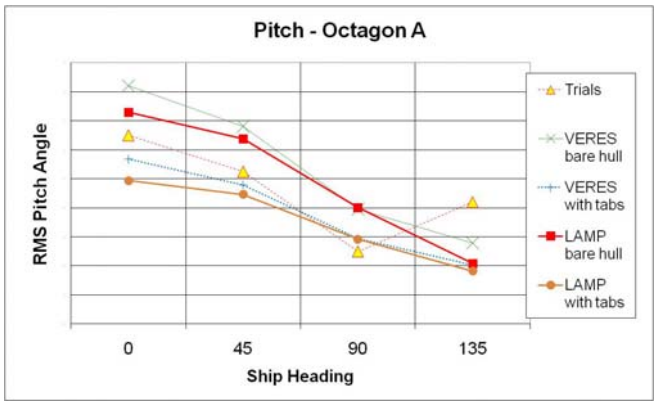


**Fig. 6.** Comparison of RMS pitch angle in Octagon A

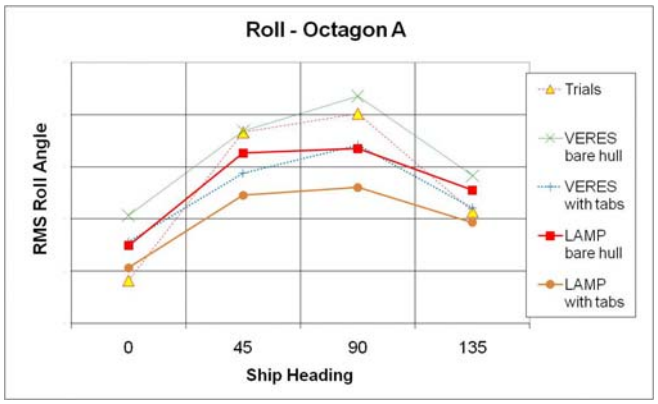


**Fig. 7.** Comparison of RMS roll angle in Octagon A

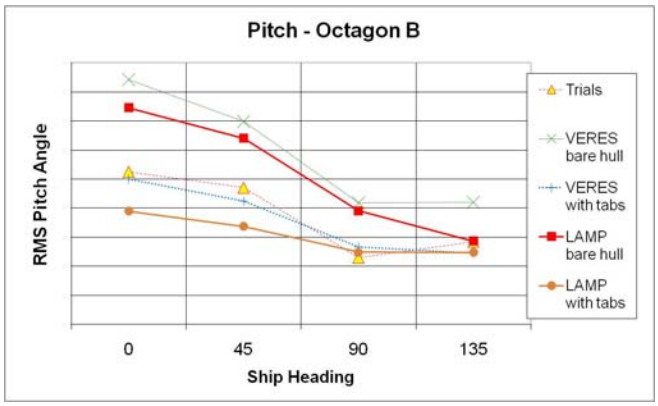


**Fig. 8.** Comparison of RMS pitch angle in Octagon B

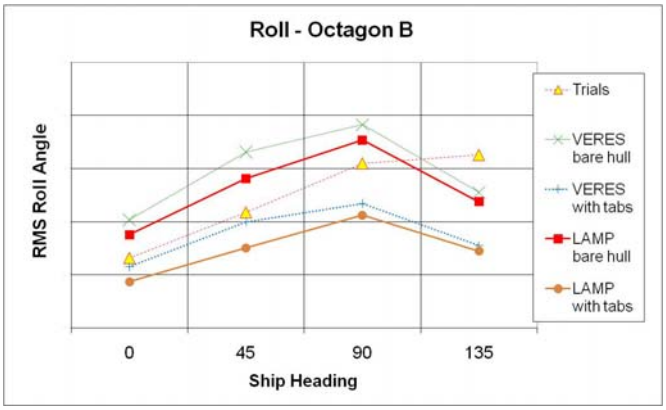


**Fig. 9.** Comparison of RMS roll angle in Octagon B

Considering the uncertainty in the measured wave field, the correlation between the LAMP predictions and the full scale trials measurements is very reasonable. The sensitivity of the calculations to the assumed values for the wave spreading function, primary wave direction is at least as large as the differences between the predictions and the trials measurements.

Some additional cases were examined with the T-foil deployed and the T-foil flaps actively controlled. The goal was to examine nearly identical octagon runs with both the trim tabs and T-foil deployed and with only the trim tabs active and the T-foil retracted out of the water. This would allow for a direct comparison of the ability of the tools to predict the influence of the T-foil. There were only a few cases during the trials for which the vessel was operated at the same speed in a similar wave spectrum with the T-foil deployed and retracted. As the sea conditions vary during the trials, no two octagons will see exactly the same wave spectrum. Two octagons were examined that were performed in succession at the same speed (35 knots) first with the T-foil deployed and then with the T-foil retracted. The wave spectra corresponding to these two octagons are shown in Figure 10. Octagon C shows the spectrum measured while the T-foil was deployed and Octagon D shows the spectrum measured while the T-foil was retracted. While the spectra are nearly the same near the peak period of around 11 seconds, there is some loss of wave energy at the secondary peak around 7 seconds. The comparison between trials results and the LAMP and VERES predictions are shown in Figure 11 for the pitch motion. Since the T-foil is mounted on the centerline of the vessel, the controller is set to reduce only the pitch motions, while the trim tabs were set to reduce both pitch and roll motions. The trials data from Octagon C show the peculiar result that the measured RMS pitch angle was higher in bow and beam seas than in head seas. This indicates perhaps that the seas were bi-directional or an error in the observed primary wave direction during the trials. Both the LAMP and VERES predictions show the expected result that both the pitch motion increases as the heading approaches head seas, and both tool predict that the greatest benefit from the T-foil is in head and bow seas. The trials indicate the T-foil has the most benefit in bow and beam seas. LAMP predicts a

slightly smaller reduction in pitch motion a due to the T-foil being deployed compared with VERES. The magnitude of the reduction in pitch motion from both tools correlates reasonably well with reduction in pitch motion due to the deployment of the T-foil observed in the trials.

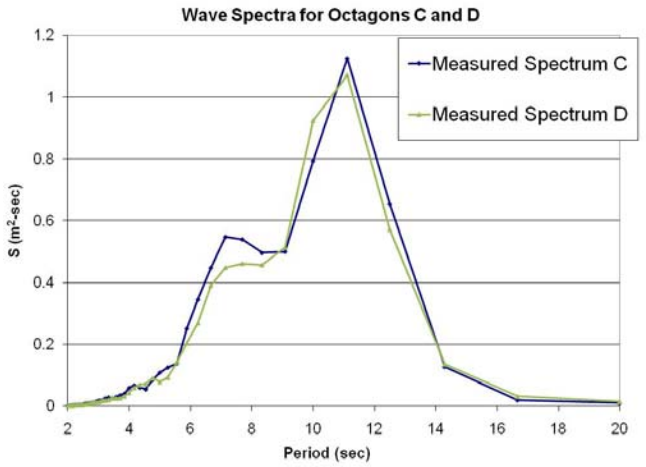


**Fig. 10.** Wave Spectra measured during Octagons C and D

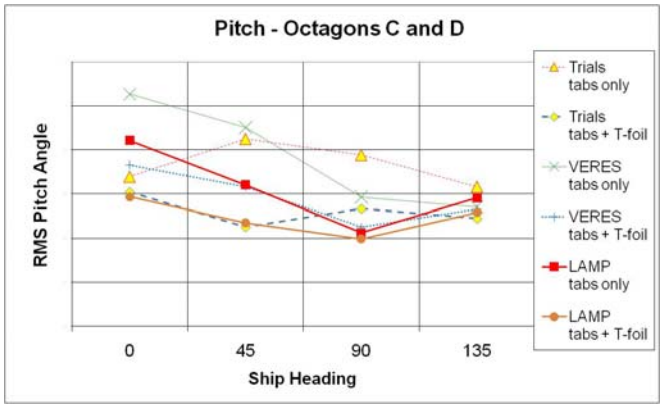


**Fig. 11.** Wave Spectra measured during Octagons C and D

## 4.0 Conclusions and Discussion

The ability of LAMP to model the RCS for a high-speed catamaran has been demonstrated. Predictions from LAMP are show for a wave piercing catamaran with an RCS consisting of trim tabs and a single center mounted T-foil. The LAMP predictions are compared both with full scale trials data and the predictions from VERES. The LAMP and VERES predictions in general correlate well with each other. The VERES calculations are purely linear, while LAMP includes a nonlinear calculation of the incident wave forcing and hydrostatic restoring forces, and LAMP includes a more accurate model for the variation in the trim tab lift with deflection angle. While it is not possible to make any quantitative statement regarding how accurately LAMP models the RCS due to limited information describing the encountered seas during the trials and a lack of trials data with the trim tabs locked in a fixed position, some qualitative conclusions can be made. Generally the LAMP predictions show a significant benefit from actively controlled trim tabs and T-foils for reducing both pitch and roll motions. For the cases examined with only the trim tabs active, LAMP shows reasonable correlation with the trials data for the predicted pitch response, but slightly under-predicts the roll motion. LAMP predicts roughly the correct magnitude for the reduction in pitch motion and bow acceleration from the T-foil. There are a variety of sources for discrepancies between the LAMP predictions and the trials data. Among these are:

- Differences in the incident wave field between the trials and LAMP predictions. There is a high degree of uncertainty in the amount wave spreading and directionality of the measured spectrum. Also in LAMP the wave spectrum is assumed to be spatially and temporally constant during an octagon maneuver, where in reality there is probably some spatial and temporal variation,
- Assumptions made concerning the control algorithm in the LAMP calculations. Perhaps the control algorithm on the actual vessel was designed to limit accelerations at specific locations instead of only reducing roll and pitch motions.
- Error in computing the lift force on the trim tabs and T-foils. VERES treats both the trim tabs and T-foil as submerged foils, assuming a lift force that is linear with the angle of attack on the foil. The angle of attack is derived from the hull motion and wave orbital velocities. Including the wave orbital velocity in angle of attack is appropriate for a submerged T-foil, but less appropriate for a trim tab flap, where the flow leading into the trim tab must be tangential to the hull.
- Errors in the LAMP predictions for the bare hull vessel response. Since there are no trials data available for the bare hull, it is not possible to determine what part of the difference between trials data and LAMP predictions should be attributed to errors in modeling the ride control system, and what should be attributed to errors in predicting the response of the bare hull.

There are many potential advantages to using a time-domain method panel method such as LAMP to model vessels with RCS.. These advantages include the ability to incorporate non-linear control algorithms and non-linear formulae for the lift force generated by trim tabs and interceptors. In addition some of the non-linear influence of the hull geometry on the hydrostatic and wave exciting forces can also be modeled in the time-domain. A model test data set for a vessel with an active RCS would be beneficial for validating simulation tools. The model test data should include runs for both the bare hull and with the RCS installed in the same wave conditions, so that the ability of the simulation tools to predict the reduction in motions due to the RCS could be directly validated.

## REFERENCES


Comstock, J. P. (ed.) (1967). Principles of Naval Architecture. The Society of Naval Architects and Marine Engineers.

Dawson D. and Blount D. (2002): "Trim Control", Professional Boatbuilder, No 75.

Faltinsen, O. M. and R. Zhao (1991): "Numerical Predictions of Ship Motions at High Forward Speed", Phil. Trans. Royal Soc. London, Vol. 334 pp. 241–252.

Fathi, Dariusz and Hoff, Jan Roger (2004): ShipX Vessel Responses (VERES) Theory Manual, February 2004.

Fathi, Dariusz (2004): ShipX Vessel Responses (VERES) Ship Motions and Global Loads, User's Manual, December 2004.

Hart, C.J., Weems, K.M., Peltzer, T.J., (2007) "Seakeeping Analysis of the Lifting Body Technology Demonstrator Sea Flyer Using Advanced Time-Domain Hydrodynamics", Ninth International Conference on Fast Sea Transportation, Shanghai, China, September 2007.

Hoerner, S.F. (1965): Fluid Dynamic Lift: Theoretical, Experimental and Statistical Information, Hoerner Fluid Dynamics

Hughes, M. J., (2010) "Seakeeping Simulations for High-Speed Vessels with Active Ride Control Systems," Seventh International Conference on High-Performance Marine Vehicles, Melbourne, Florida, USA, 13-15 October 2010.

Lewandowki, E. M. (2004), The Dynamics of Marine Craft: Maneuvering and Seakeeping, World Scientific Publishing Co., Singapore

MDI (2003a): Maritime Dynamics, Inc., Technical Memorandum MD-R-2836-02, Rev A. "Seakeeping Predictions for Center for Innovation in Ship Design 86M Catamaran."

MDI (2003b): Maritime Dynamics, Inc. Technical Memorandum MD-R-2836-01, "Catamaran Seakeeping Simulation Program Background Introduction and Briefing"

O'Dea, John (2005): "Correlation of VERES Predictions for Multihull Ship Motions" NSWCCD-50-TR-2005/021 Sept 2005.

Salvesen, N., E. O. Tuck and O. Faltinsen (1970): "Ship Motions and Sea Loads", Transactions SNAME, Vol. 78, pp. 250–287.

Shin, Y.-S., Belenky, V. L., Lin, W.-M., Weems, K. M., Belknap, W. F., & Engle, A. H. (2003). 'Nonlinear Time Domain Simulation Technology for Seakeeping and Wave Load Analysis for Modern Ship Design.' Transactions SNAME, 111, pp. 557-578.

Stern, F., Carrica, P., Kandasamy, M., Gorski, J., O'Dea, J., Hughes, M., Miller, R., Kring, D., Milewski, W., Hoffman, R., & Cary, C. (2006): 'Computational Hydrodynamic Tools for High-Speed Sealift'. Transactions SNAME, Vol. 114.

Villa, D. and Brizzolara, S. (2009): "A Systematic CFD Analysis of Flaps / Interceptors Hydrodynamic Performance", Proc. Tenth International Conference on Fast Sea Transportation (FAST 2009), Athens, Greece, pp. 1023-1038

von Mises, R. (1945). Theory of Flight. Dover Publication, Toronto, Canada

Zhang, S., Weems, K.M. and Lin, W.M. (2003): "A Validation Study of the Large Amplitude Motion Program (LAMP) for a High-Speed Catamaran - Delft Catamaran 372," SAIC Report 03-1042.

Zhang, S., Weems, K.M., and Lin, W.M. (2009): "Investigation of the Horizontal Drifting Effects on Ships with Forward Speed," Proceedings of the ASME 28th International Conference on Ocean, Offshore and Arctic Engineering (OMAE2009), Honolulu, Hawaii.


## ACKNOWLEDGEMENTS


The authors would like to thank Dr. John Barkyoumb and the Naval Innovative Science and Engineering Program at NSWCCD for support of this work. The authors would also like to thank Ben Schaub from Naiad Dynamics, Inc. for his guidance and advice on modeling ride control systems and Robert Bachman and Matthew Powell from the Seakeeping Division at NSWCCD for their assistance providing and understanding the full-scale trials data.